

# Wide-angle vertical coupling gratings enabled by nano-imprinted microlens array

Gan Xiao,<sup>1,2,3</sup> Xuanming Zhang,<sup>4</sup> Fei Lou,<sup>4</sup> Lei Lei,<sup>1,2,3,\*</sup> and Xin Cheng<sup>4</sup>

<sup>1</sup>State Key Laboratory of Radio Frequency Heterogeneous Integration (Shenzhen University)

<sup>2</sup>Key Laboratory of Optoelectronic Devices and Systems of Ministry of Education and Guangdong Province, Shenzhen 518060, China

<sup>3</sup>College of Physics and Optoelectronic Engineering, Shenzhen University, Shenzhen 518060, China

<sup>4</sup>Department of Materials Science and Engineering, Southern University of Science and Technology Shenzhen, China

\*leilei@szu.edu.cn

**Abstract:** We experimentally show a vertical grating coupler featuring extended coupling angles through nano-imprinted lens array. This nanostructure exhibits a 2-3.4 dB increase in coupling efficiency within the  $\pm 15^\circ$  angular range compared to the bare device. © 2024 The Author(s)

## 1. Introduction

Photonic integrated circuits (PICs) hold significant potential to enable a diverse array of applications, including but not limited to data communication [1], biosensing [2], positioning and navigation [3], spectroscopy, signal processing, quantum communication, and beyond. However, efficient coupling from the external optical fiber to the chip is always a challenge. For grating couplers (GCs), the application of perfectly vertical coupler is more attractive than non-vertical coupler due to the less difficulties of the alignment and packaging [4], thus allowing high-density integration. Moreover, in specific scenarios, particularly in cytometry, capturing a broad-spectrum, wide-angle scattered signal from a target is essential for precise particle or cell size measurements [5]. These measurements provide crucial insights into organelles and are indispensable. However, it's worth noting that the light scattered by the analyte can strike the detector or coupler at various angles, including regular and oblique incidences, often with unpredictable angles of incidence. In such cases, employing an optical waveguide or fiber that can accommodate a wide field of view proves advantageous in reducing scattered light losses and alleviating stringent alignment requirements, thus enabling efficient real-time sensing. Much of the research focus lies in enhancing coupling efficiency at specific incident angles, primarily due to the narrow full width at half maximum (FWHM), leaving minimal tolerance for angular deviations. Consequently, precise alignment becomes imperative, as any deviation from the designated angle results in a sharp decline in coupling efficiency.

In this paper, we introduce a silicon GC for vertical coupling with a wide incident angle range. Our approach utilizes nanoimprinting technology to create a microlens array integrated into a single silicon photonic integrated chip [6]. This hybrid integration affords greater flexibility in manipulating the light field, thus enabling a wider field-of-view angle. A vertically-coupled, fully etched chirped grating coupler was fabricated using standard silicon-on-insulator (SOI) process. Employing nanoimprint technology, a 3  $\mu\text{m}$ -diameter microlens array was successfully imprinted onto the coupler. Based on the lens-array assisted GC, the coupling efficiency under  $-15^\circ$  to  $15^\circ$  incident angle range rises of 2-3.4 dB compared to that of the bare GC, which in turn shows that the proposed nanostructure owns a much wider field-of-view under the same coupling efficiency. Moreover, the coupling bandwidth broadens more than 30 nm. This wide-angle ability for vertical coupling holds significant potential applications in high-performance optical detection, real-time biochemical sensing, and more.

## 2. Design and fabrication

The device comprises a 220 nm fully etched chirped grating and a nanoimprinted microlens array. As depicted in Fig. 1(a), the initial grating etching width is  $w_0=120$  nm, with a width variation of  $\Delta w=30$  nm and a grating period of  $P=700$  nm. The hemispherical lens array is based on a 20  $\mu\text{m}$  thick polymer and features a 3  $\mu\text{m}$  diameter. At a wavelength of 1550 nm, simulation results in Fig. 1(b) clearly illustrates that the inclusion of the microlens array well improves the overall coupling efficiency within the same coupling angle range. In other words, while maintaining the same level of coupling efficiency, our proposed hybrid integration nanostructure largely broadens the field of view angle of the vertical grating coupler. Fig. 1(c) provides a comparison involving shifts in the position of the imprinted microlens array. Notably, the device's performance remains nearly unaffected even with a lens array offset of 1-2  $\mu\text{m}$ , effectively mitigating the impact of lens position errors on the device's coupling performance. The silicon chirped grating is fabricated through a standard SOI process, involving electron beam

lithography (EBL) and inductively coupled plasma (ICP) etching. The nanoimprinted microlens array is created on a polyethylene terephthalate (PET) film, as depicted in Fig. 1(d). The subtemplate1 is initially generated on the resist PAM400 by imprinting a converted hemispherical silicon mold with a diameter of  $3\ \mu\text{m}$  created by laser direct writing lithography (step a). After that, a UV curable resist PAPI100 is spin-coated on another PET film, and subtemplate1 is stamped on PAPI100 to produce the subtemplate2 through UV nanoimprinting (step b). Subsequently, a  $20\ \mu\text{m}$  thick PAM400 is applied through spin-coating onto the chirped GC, followed by compression using subtemplate2 and exposure to ultraviolet irradiation (step c). Fig. 1(e) presents the SEM image of the lens array, which shows good agreement with the design.

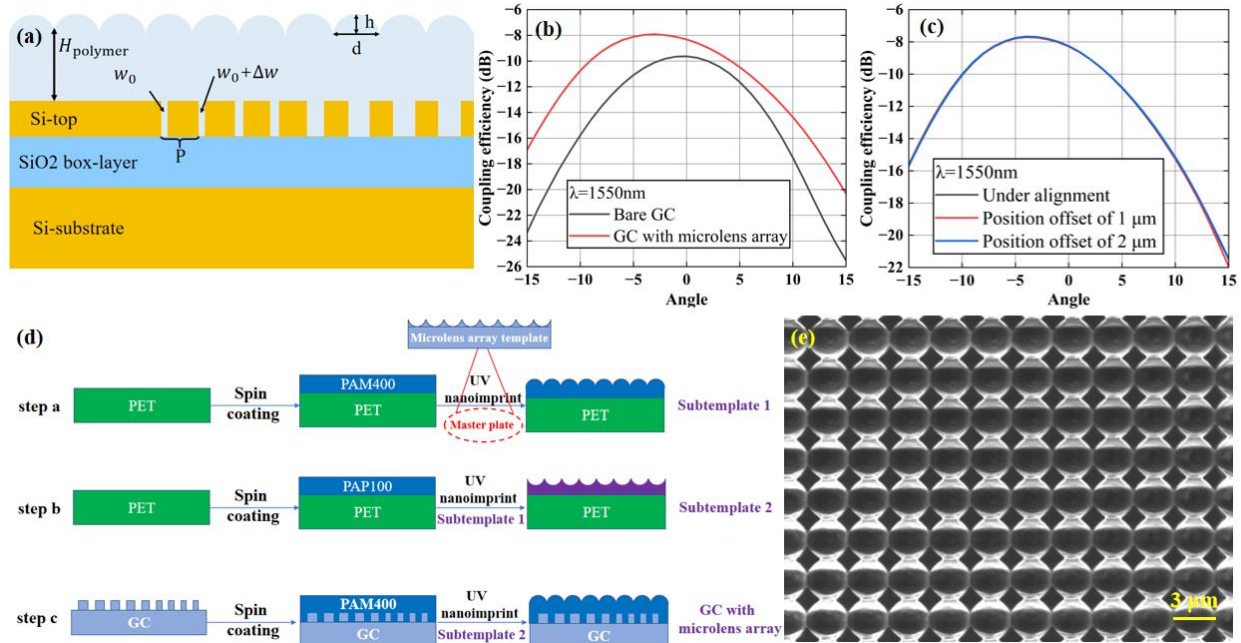


Fig.1. (a) Device structure. (b) Comparison of the coupling efficiency as a function of coupling angle of GCs without and with microlens array. (c) Coupling efficiency as a function of coupling angle under different microlens position offsets. (d) Flow chart of nanoimprinted lens array. (e) SEM image of the fabricated microlens array.

### 3. Measurements

The experimental setup depicted in Fig. 2(a) involves a tunable continuous wave (CW) laser operating at  $1550\ \text{nm}$ , followed by a polarization controller for optimizing coupling polarization. We use both optical power meter and spectrometer to evaluate the coupling performance. Fig. 2(b) compares the coupling efficiency of the device as a

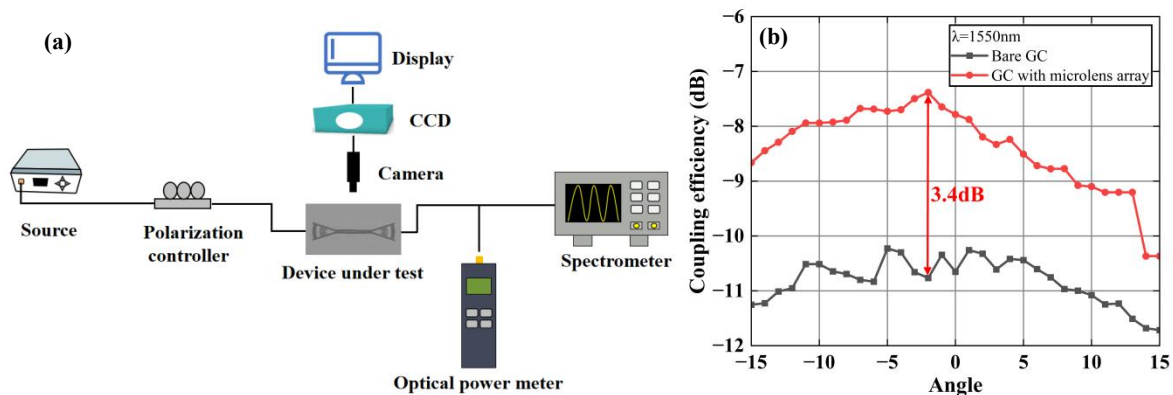


Fig.2. (a) Experimental setup. (b) Comparison of coupling efficiency between bare GC and GC with microlens array.

function of the incident angle before and after integrating the microlens array. Overall, the microlens array-assisted GC shows a noticeable improvement in the average coupling efficiency as the incidence angle increases. Specifically, we observe an increase of over 3 dB in proximity to normal incidence. An optical coupling efficiency of

-7.32 dB/facet is attained at  $-2^\circ$ , effectively considered as a normal incidence. This slight angular deflection is attributed to the effective refractive index change induced by the polymer microlens array.

To further explore the bandwidth characteristics of the wide-angle vertical GC, we analyze the angular spectra as depicted in Fig. 3. It becomes evident that the integration of the nanoimprinted microlens array results in a substantial broadening of the coupling bandwidth within the C-band. With a benchmark of -9 dB/facet, the proposed device demonstrates a notable extension of over 30 nm in its vertical coupling bandwidth, while consistently maintaining robust coupling performance across a  $\pm 15^\circ$  angular range. Both Fig. 2 and Fig. 3 clearly illustrate the microlens array's ability to efficiently converge incident light, effectively converting a wide range of incident angles into angles conducive to vertical coupling with the grating. This, in turn, significantly extends the overall incident angle range of the device.

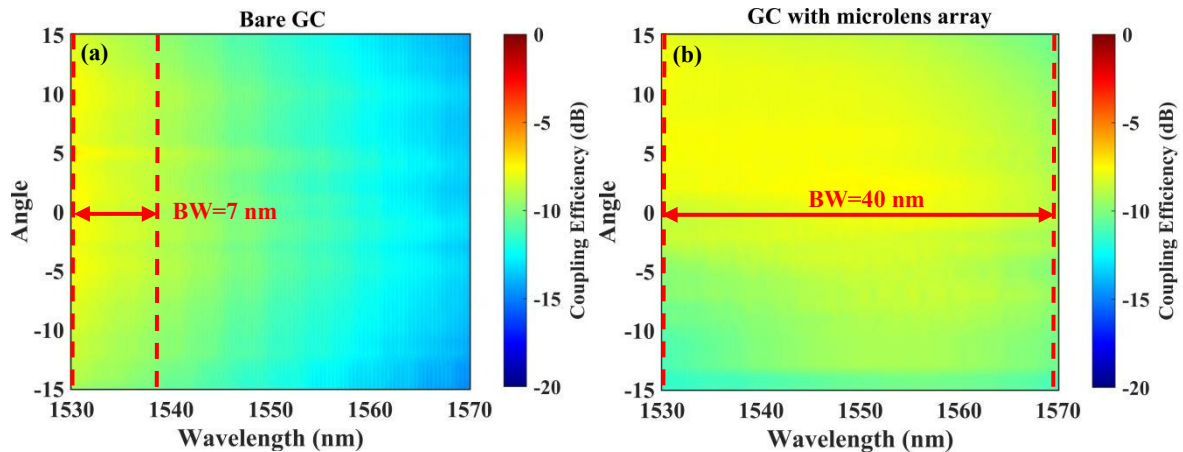


Fig.3. Comparison of the angular spectra between GC and GC with microlens array.

#### 4. Conclusion

We propose and experimentally demonstrate a wide-angle grating coupler designed for vertical coupling, achieved through the hybrid integration of a nanoimprinted microlens array with a chirped grating. The microlens array effectively manipulates the incident angle to align with the vertical grating coupler's range, thus extending field-of-view angle for the entire device. Moreover, the use of this array feature significantly mitigates the challenges associated with the alignment between the microlens array and the silicon device, offering improved fabrication error tolerance. In terms of coupling performance, the lens-array assisted GC exhibits a 2-3.4 dB increase in coupling efficiency within the  $-15^\circ$  to  $15^\circ$  range compared to the bare GC. Essentially, the lens-array assisted GC provides a broader field of view angle range while maintaining the same level of coupling efficiency. Furthermore, this method achieves a great bandwidth extension of over 30 nm within the  $\pm 15^\circ$  angular range. In addition to the lens array, the enhancement of the incidence angular range is highly feasible through the incorporation of other nanoimprinted structures, including metalens, microprism, and an additional layer of grating. The proposed nanostructure exhibits substantial promise for applications in high-performance optical detection and real-time biochemical sensing.

#### 5. References

- [1] Li X, Liu H, Wang W, et al. Big data analysis of the internet of things in the digital twins of smart city based on deep learning[J]. *Future Generation Computer Systems*, 2022, 128: 167-177.
- [2] Rong G, Corrie S R, Clark H A. In vivo biosensing: progress and perspectives[J]. *ACS sensors*, 2017, 2(3): 327-338.
- [3] El-Sheimy N, Li Y. Indoor navigation: State of the art and future trends[J]. *Satellite Navigation*, 2021, 2(1): 1-23.
- [4] Orlando A, Franceschini F, Muscas C, et al. A comprehensive review on Raman spectroscopy applications[J]. *Chemosensors*, 2021, 9(9) 262.
- [5] Kumari S, Saha U, Bose M, et al. Microfluidic Platforms for Single Cell Analysis: Applications in Cellular Manipulation and Optical Biosensing[J]. *Chemosensors*, 2023, 11(2): 107.
- [6] Unno N, Mäkelä T. Thermal nanoimprint lithography—a review of the process, mold fabrication, and material[J]. *Nanomaterials*, 2023, 13(14): 2021.